Anti-human ACE2 antibody neutralizes and inhibits virus production of SARS-CoV-2 variants of concern

Chaouat, Abigael E.; Brizić, Ilija; Kučan Brlić, Paola; Atari, Nofar; Kliker, Limor; Alfi, Or; Mandelboim, Michal; Wolf, Dana; Tafish, Laith; Kol, Inbal; ...

Source / Izvornik: **iScience, 2022, 25**

Journal article, Published version
Rad u časopisu, Objavljena verzija rada (izdavačev PDF)

https://doi.org/10.1016/j.isci.2022.104935

Permanent link / Trajna poveznica: https://urn.nsk.hr/urn:nbn:hr:184:257342

iScience

CellPress
OPEN ACCESS

Article

Anti-human ACE2 antibody neutralizes and inhibits virus production of SARS-CoV-2 variants of concern

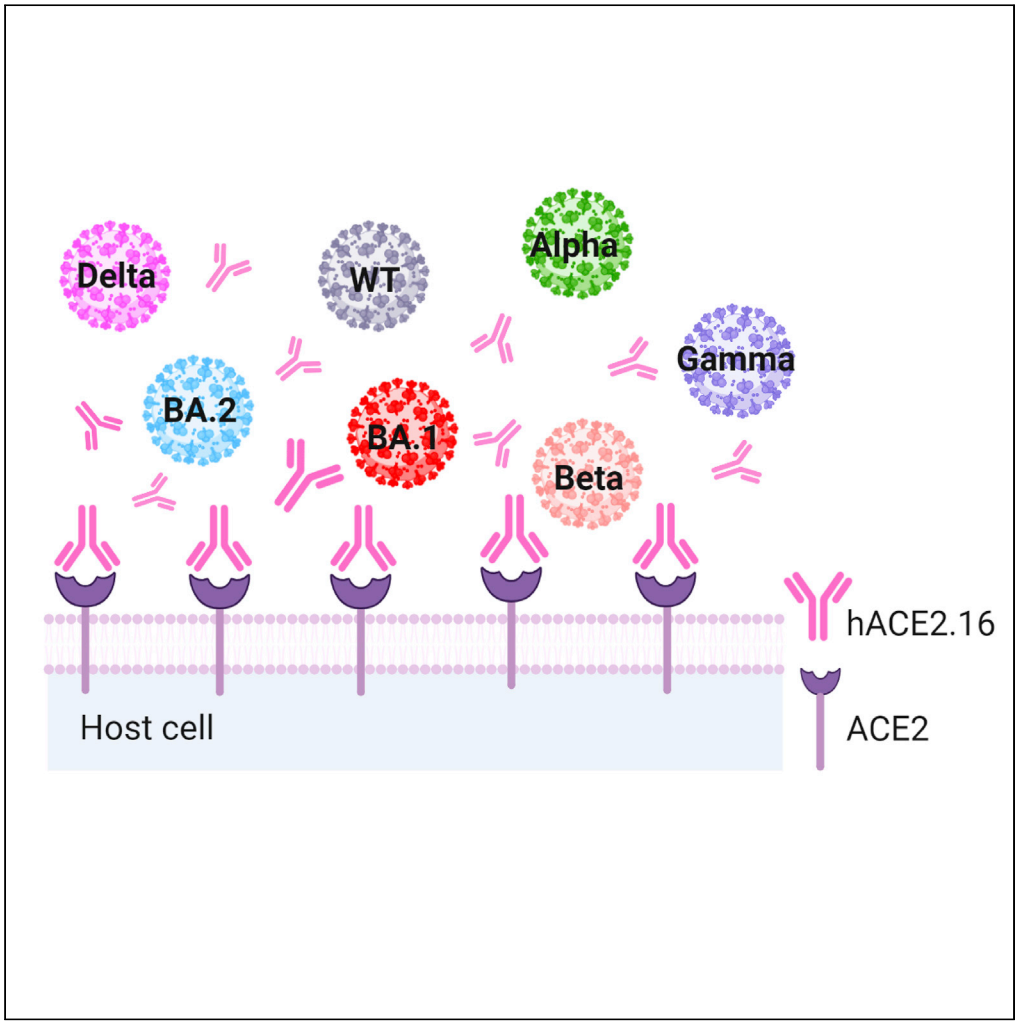

Abigael E. Chaouat, Ilija Brizic, Paola Kucan Brlic, ..., Inbal Kol, Stipan Jonjic, Ofer Mandelboim

oferm@ekmd.huji.ac.il

Highlights

We develop a specific antibody against human ACE2 named hACE2.16

hACE2.16 does not interfere with ACE2 activity

hACE2.16 blocks infection and virus production of SARS-CoV-2 VOCs

Chaouat et al., iScience 25, 104935
September 16, 2022
https://doi.org/10.1016/j.isci.2022.104935

iScience

CellPress
OPEN ACCESS

Article

Anti-human ACE2 antibody neutralizes and inhibits virus production of SARS-CoV-2 variants of concern

Abigael E. Chaouat,[1,6] Ilija Brizic,[2,6] Paola Kucan Brlic,[2,6] Nofar Atari,[3] Limor Kliker,[3] Or Alfi,[1] Michal Mandelboim,[3,4] Dana Wolf,[1,5] Laith Tafish,[1] Inbal Kol,[1] Stipan Jonjic,[2,7] and Ofer Mandelboim[1,7,8,*]

SUMMARY

The global pandemic caused by SARS-CoV-2 is a major public health problem. Virus entry occurs via binding to ACE2. Five SARS-CoV-2 variants of concern (VOCs) were reported so far, all having immune escape characteristics. Infection with the current VOC Omicron was noticed in immunized and recovered individuals; therefore, the development of new treatments against VOC infections is urgently needed. Most approved mAbs treatments against SARS-CoV-2 are directed against the spike protein of the original virus and are therefore inefficient against Omicron. Here, we report on the generation of hACE2.16, an anti-ACE2 antibody that recognizes and blocks ACE2-RBD binding without affecting ACE2 enzymatic activity. We demonstrate that hACE2.16 binding to ACE2 does not affect its surface expression and that hACE2.16 blocks infection and virus production of various VOCs including Omicron BA.1 and BA.2. hACE2.16 might, therefore, be an efficient treatment against all VOCs, the current and probably also future ones.

INTRODUCTION

SARS-CoV-2 (severe acute respiratory syndrome coronavirus 2) was first reported in December 2019 in China. It is a highly contagious virus that leads to COVID-19 (coronavirus disease 2019), a potentially fatal disease. Since its appearance, SARS-CoV-2 is an ongoing threat to humanity. Currently, ~500 million people were infected, from which more than 6 million died (World Health Organization, 2022). Infection starts when the RBD (receptor-binding domain) of the spike protein binds to the ACE2 (Angiotensin Converting Enzyme-2) receptor found on host cells (Wang et al., 2020), and ends by the release of virions that binds to ACE2 receptors elsewhere (Loganathan et al., 2021). ACE2 is a transmembrane glycoprotein enzyme involved in many important physiological processes. It plays a role in the renin-angiotensin hormone system by transforming ANG II to protective ANG (1–7), as well as a regulator of blood volume, stem cell maintenance and differentiation, hematopoiesis, erythropoiesis, myeloid differentiation, inflammation, and innate and adaptive immunity (Triposkiadis et al., 2021; Wang et al., 2016). ACE2 is highly expressed in the brain, cardiomyocytes, kidneys, intestines, and male reproduction organs (Zhou et al., 2020). As a transmembrane protein, it contains a signal peptide at the N-terminal, a metalloproteinase active site, a transmembrane domain, and a short cytoplasmic domain at the C-terminus (Wu et al., 2021).

Since the pandemic had begun, the virus evolved, and concerning mutations that occurred mainly in the SARS-CoV-2 spike protein had led to the development of five VOCs. The first classified VOC was named Alpha (B.1.1.7). Mutations in the Alpha spike protein (especially N501Y) increased its binding affinity to ACE2 and consequently increased virus replication in human upper-airway cells (Laffeber et al., 2021). Beta (B.1.351) and Gamma (P.1) VOC have the combination of N501Y, E484K, and K417N mutations in the RBD. Although the N501Y and E484K mutation enhance the affinity to ACE2, K417N attenuates it (Tao et al., 2021). The E484K mutation also confers resistance to neutralization by several mAbs which targets the RBD (Wang et al., 2021) as well as reduced susceptibility to plasma samples from people immunized with one of the authorized mRNA vaccines (Zhang et al., 2021). The Delta variant (B.1.617.2) contains 4 additional mutations in the RBD and is therefore inefficiently neutralized by most BNT162b2-immune sera (Liu et al., 2021a, 2021b). Omicron (B.1.1.529), the fifth VOC was detected in South Africa at the end of November 2021. Currently, Omicron has five sub-lineages: BA.1-5 (World Health Organization, 2022).

[1]The Concern Foundation Laboratories at the Lautenberg Center for Immunology and Cancer Research, Institute for Medical Research Israel Canada (IMRIC), The Hebrew University Hadassah Medical School, Ein Karem, Jerusalem 9112001, Israel

[2]Center for Proteomics University of Rijeka, Faculty of Medicine, Brace Branchetta 20, 51000 Rijeka, Croatia

[3]Central Virology Laboratory, Public Health Services, Ministry of Health and Sheba Medical Center, Sheba Medical Center Hospital- Tel Hashomer, Ramat Gan 52621, Israel

[4]Sackler Faculty of Medicine, Tel Aviv University, Tel Aviv 6997801, Israel

[5]The Hebrew University, Hadassah Medical Center, Ein Karem, Jerusalem 9112001, Israel

[6]These authors contributed equally

[7]These authors contributed equally

[8]Lead contact

*Correspondence: oferm@ekmd.huji.ac.il

https://doi.org/10.1016/j.isci.2022.104935

The BA.1 sub-variant contains 35 mutations in its spike protein, 23 of which are unique to this variant (Kannan et al., 2022). Moreover, out of the 35 spike mutations, 15 are located in the RBD of the spike protein (Lupala et al., 2022), a major target of neutralizing antibodies (NAbs) (Harvey et al., 2021). Although BA.2 is an omicron descendant, its genomic sequence is heavily different from that of BA.1 (Yamasoba et al., 2022a). The BA.4 and BA.5 subvariants which appeared in South Africa in January 2022 were reclassified from variants of interest to variants of concern in May 2022, as they have become dominant around the globe (European Centre for Disease Prevention and Control, 2022). Most importantly, all Omicron subvariants can escape vaccine-elicited antibodies, convalescent antibodies, or both as well as most of the mAbs in clinical use (Liu et al., 2021a, 2021b; Lu et al., 2021; Pulliam et al., 2021; Rössler et al., 2022; Sheward et al., 2022; Tuekprakhon et al., 2022b; Yamasoba et al., 2022a).

As the binding of the spike protein to the ACE2 receptor is critical for SARS-CoV-2 infection, blocking it may help to treat infection. Indeed, most prophylactic and therapeutic treatments target the spike protein.

To try to stop the pandemic, the FDA initially issued an emergency use authorization (EUA) for Pfizer (Administration, 2020a) and Moderna (Administration, 2020b) vaccines. Both vaccines are composed of a lipid-nanoparticle encapsulated mRNA expressing the prefusion-stabilized spike glycoprotein of the original SARS-CoV-2 (Baden et al., 2021; Polack et al., 2020). Then, three anti-SARS-CoV-2 mAbs (monoclonal antibodies) received a EUA from the FDA. Bamlanivimab and Etesevimab neutralizing mAbs that target the spike glycoprotein of SARS-CoV-2 are given together to treat infection (Dougan et al., 2021). REGN-COV2 is another combination of two monoclonal antibodies (casirivimab and imdevimab) that bind to non-overlapping epitopes of SARS-CoV-2 RBD (Group et al., 2021). However, the administration of these antibodies was stopped as the current Omicron VOC has markedly reduced susceptibility to both treatments (National Institutes of Health, 2021). Sotrovimab is another antibody that was firstly isolated from a SARS survivor, it recognizes a conserved binding site on SARS-CoV-2 spike protein (Gupta et al., 2021). As it targets a conserved binding site it was believed that it may retain its neutralizing against all variants but it was recently published that a 16-fold change in IC50 was observed for the Omicron BA.2 variant (Cathcart et al., 2022). As a result of that, the FDA decided to limit the use of Sotrovimab (FDA, 2022). Only two current given treatments have EUA: Bebtelovimab and Evusheld (AZD7442). Both treatments target the spike protein of SARS-CoV-2 but while AZD7442 (Levin et al., 2022) consists of two monoclonal antibodies with modified Fc fragments so that they would have an extended half-life and decreased immune effector functions, Bebtelovimab (U.S. Food and Drug Administration, 2021) is unmodified in its Fc region. Bebtelovimab potently neutralizes Omicron BA.2 (Westendorf et al., 2022) and BA.4/5 (Cao et al., 2022). It has been recently suggested that the neutralizing activity of AZD7442 against the BA.2 sub-variant is only minimally lower than the wild-type virus (Levin et al., 2022). As for BA.4/5, the activity of AZD7442 was reduced 8.1-fold compared with BA.2 (Dong et al., 2021).

The increased resistance to the spike-targeted Abs observed with the development of the VOCs suggests that the spike protein evolves rapidly to evade immunity, emphasizing the need for the development of novel treatments.

RESULTS

Generation of 293T-ACE2 cells

To develop an efficient treatment against all VOCs we decided to generate a blocking antibody against ACE2. We hypothesized that as ACE2 is not mutating or dramatically changing its expression during infection, a blocking antibody against ACE2 will block the infection of all VOCs.

To test for specific recognition of the generated antibodies against ACE2, we generated 293T-ACE2 cells overexpressing ACE2. We used a lentivirus expression vector and inserted an ACE2 cDNA, labeled with a FLAG tag at its N-terminus. The lentiviral vector also contains GFP. 293T cells were successfully transduced with the generated lentiviral vector as the transduced cells express both GFP (Figure 1A) and were stained positively with an anti-flag-Tag antibody (Figure 1b). In contrast, parental cells were flag-Tag negative (Figure 1B). To further verify ACE2 expression we used a commercial anti-ACE2 antibody. We stained the 293T-parental and 293T-ACE2 cells, and as expected, ACE2 expression was detected on the 293T-ACE2 cells, while minimal staining was observed on the parental 293T cells (Figure 1C).

We next tested whether the commercial anti-ACE2 antibody can block the binding of RBD to ACE2. For that, we used a fusion protein of SARS-CoV-2 wild-type receptor binding domain (RBD) which we have

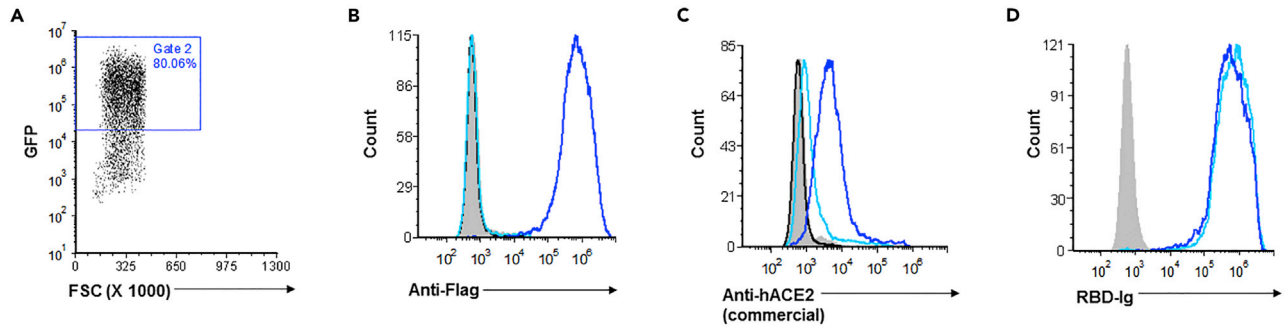

Figure 1. Generation of 293T cells expressing ACE2

(A) GFP expression in 293T-ACE2 cells.

(B and C) 293T parental cells (light blue) and 293T-ACE2 cells (dark blue) were stained with either anti-Flag tag antibody (B) or with an anti-human ACE2 commercial antibody (C). Black histograms represent the background staining of 293T parental cells and gray-filled histograms represents background staining of 293T-ACE2 cells.

(D) RBD-Ig staining following incubation with commercial antibody (light blue) or without antibody (dark blue). Representative of 3 experiments.

generated previously and demonstrated that it binds ACE2 (Chaouat et al., 2021). We incubated 293T-ACE2 cells with or without the commercial antibody and then stained the cells with RBD-Ig. As can be seen, similar levels of RBD-Ig staining were observed, irrespectively of whether the antibody was present or not (Figure 1D).

Thus, we have generated 293T cells expressing ACE2, demonstrated that ACE2 is recognized by RBD-Ig and that the commercial anti-ACE2 antibody cannot block this interaction.

hACE2.16 antibody binds human ACE2 specifically and blocks SARS-CoV-2 RBD binding

To generate anti-ACE2 antibodies we immunized mice with an ACE2-Ig fusion protein that we have generated previously (Chaouat et al., 2021). We used a fusion protein of ACE2 because our fusion protein contains only the extracellular portion of ACE2 and because it enables efficient purification using protein A/G columns (Harper and Speicher, 1997). Moreover, the Fc fragment increases the half-life of the protein (Beck and Reichert, 2011).

Following ACE2-Ig immunization, we obtained mAbs that recognized ACE2-Ig specifically. Nine of these antibodies were able to recognize ACE2 expressed on 293T, but not the parental 293T cells, to various degrees (Figure 2A).

Next, to assess whether one or more of these antibodies may block SARS-CoV-2 RBD-Ig binding we incubated 293T-ACE2 cells with or without hybridoma supernatants obtained from the above-mentioned 9 anti-ACE2 antibodies and then stained all cells with RBD-Ig. Only one antibody; anti-hACE2.16, was able to block RBD-Ig binding (Figure 2B).

We next purified the hACE2.16 antibody and used various concentrations of the antibody (4-100 ug/mL) and incubated them with the 293T-ACE2 cells. We next stained the cells with RBD-Ig staining.

As can be seen, hACE2.16 efficiently blocked RBD-Ig binding in a dose-dependent manner (Figure 2C).

hACE2.16 antibody does not affect ACE2 enzymatic activity and does not lead to ACE2 internalization

One of the well-known functions of ACE2 is the hydrolysis of angiotensin II (1-7). Thus, it was important to test whether hACE2.16 may affect the enzymatic activity of ACE2. To test it, 293T-ACE2 lysates were incubated with different αhACE2 antibodies (Figure 3A). The ACE2 activity was determined by a commercial kit (see STAR Methods) in which an ACE2 fluorogenic peptide substrate (Mca-YVADAPK(Dnp)-OH) is added and fluorescence was monitored by a plate reader. The fluorescence levels, which indicate ACE2 activity, are represented as mean RFU (relative fluorescence unit). Necl.01 (an antibody against Necl-3 also produced by hybridoma cells) was used as a control.

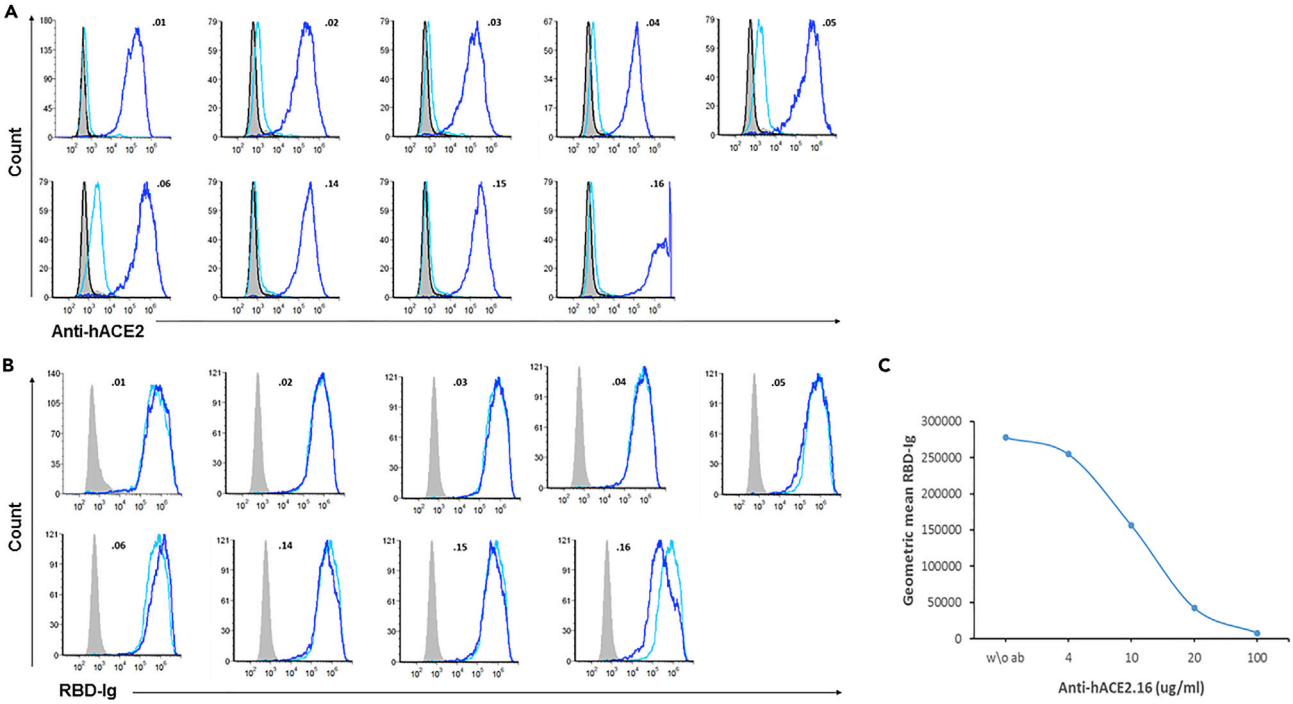

Figure 2. Anti-hACE2.16 antibody recognizes ACE2 and blocks RBD-Ig binding

(A and B) Various anti-ACE2 antibodies (antibody number indicated in each histogram) were analyzed by flow cytometry. Staining was performed on 293T-ACE2 cells (dark blue histogram) and 293T-Parental cells (light blue). Black histograms represent the background staining of 293T parental cells and gray-filled histograms represent the background staining of 293T-ACE2 cells. (B) 293T-ACE2 cells were incubated with hybridoma supernatants (dark blue) or without antibody (light blue) and then stained with RBD-Ig.

(C) 293T-ACE2 cells were incubated with increasing concentration of hACE2.16 (2-100 ug/mL), or without antibody (w\o ab), followed by RBD-Ig staining. The geometric mean of the fluorescence intensity of the staining is shown on the Y axis. Representative of 3 experiments.

As can be seen in Figure 3A, the enzymatic activity of ACE2 increased over time. Importantly, none of the anti-ACE2 antibodies, including hACE2.16 was able to block its activity.

As hACE2.16 was the only antibody able to block RBD-Ig binding, we wanted to further confirm that hACE2.16 does not affect ACE2 activity. We, therefore, repeated the experiment shown in Figure 3A using purified hACE2.16 with additional controls: anti-NKp46 antibody, commercial anti-ACE2 antibody, and another purified anti-ACE2 antibody: hACE2.01, that was unable to block RBD-Ig binding (Figure 2B). Lysate of untreated 293T-ACE2 cells were included as another control. As can be seen, none of the antibodies used was able to block ACE2 activity (Figure 3B).

Anti-ACE2 antibody might also inhibit infection by SARS-CoV-2 if the binding of the antibody will lead to ACE2 internalization. We, therefore, next test if hACE2.16 binding to ACE2 will lead to ACE2 internalization. We incubated hACE2.16 with 293T-ACE2 cells for 1,2,4,8 and 24 h at 37ºC followed by secondary antibody staining. Then, we compared the flow cytometry results to time zero in which hACE2.16 was incubated with 293T-ACE2 cells for 30 min on ice followed by secondary antibody staining. As can be seen, little or no change in the expression of ACE2 was observed, even after 24h (Figure 3C).

hACE2.16 abolish SARS-CoV-2 virus production in VERO E6 and Calu-3 cells

We next tested whether the hACE2.16 antibody can block infection using a micro-neutralization assay performed in VERO E6 cells. For that, we first tested whether our hACE2.16 can also recognize ACE2 expressed on VERO E6 monkey cells and observed that it does (Figure 4A). Then, VERO E6 cells were incubated with increasing concentrations (0.1-100 ug/mL) of hACE2.16 or with a control antibody. Subsequently, cells were infected with different VOCs; wild-type (WT), Alpha, Beta, Gamma, Delta, or Omicron (BA.1 and BA.2). Five days later, supernatants were collected and virus copy numbers were determined by RT-qPCR. We

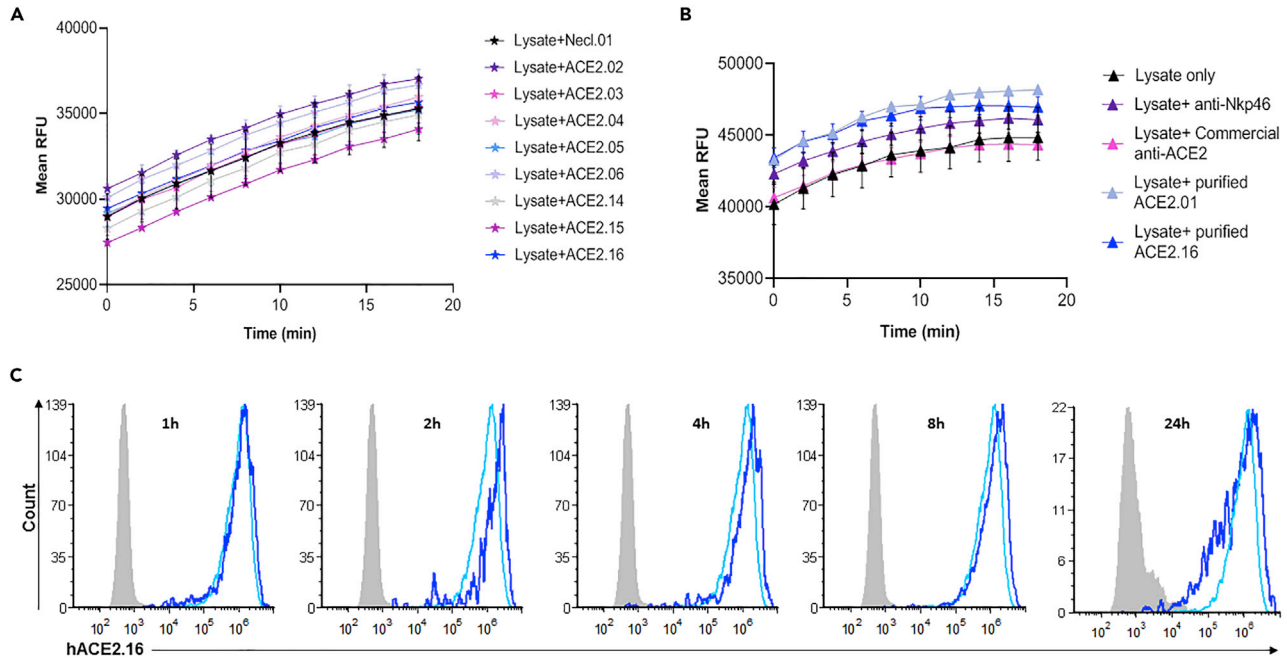

Figure 3. hACE2.16 does not affect ACE2 enzymatic and does not leads to ACE2 internalization

(A and B) Enzymatic activity of 293T-ACE2 lysates incubated with various hybridoma supernatants (A) or purified hACE2 antibodies (B). The fluorescence levels which indicate ACE2 activity are represented as mean RFU (Relative Fluorescence Unit). Necl.01 (A), anti-NKp46, commercial anti-ACE2 antibody and lysate only (B) were used as controls. Fluorescence (Ex/Em 320/420 nm) was measured in a kinetic mode (0-20 min).

(C) FACS analysis of 293T-ACE2 cells incubated with hACE2.16 time 0 on ice (light blue histogram) or after 1/2/4/8/24 h (dark blue histogram). Gray histogram represent the background staining of 293T-ACE2 cells incubated with secondary antibody only. Representative of 3 experiments.

observed a dose-dependent inhibition of virus production (Figure 4B). Importantly, 20 ug/mL and above of hACE2.16 abolished virus production of all VOCs (Figure 4B). Neutralization percentages are presented in Figure 4C along with IC50 (ug/mL). The IC50 was more or less equivalent for all VOCs, except for Beta (Figure 4C).

Vero E6 cells are monkey cells and do not express the serine protease TMPRSS2 which plays an important role in SARS-CoV-2 infection (Bestle et al., 2020). Therefore, to strengthen our results and to test the effect of hACE2.16 in a more relevant system, we repeated the micro-neutralization assay in Calu-3 cells, a human lung epithelial cell line that express ACE2 and the serine protease TMPRSS2 (Bestle et al., 2020).

We first evaluated by flow cytometry binding of hACE2.16 to Calu-3 cells as compared to a commercial anti-ACE2 antibody (Figure 4D) and saw better binding of hACE2.16 (although we used the same concentration of both antibodies).

We then repeated the experiment in Calu-3 cells using the same experimental conditions described in Figure 4. The dose-dependent inhibition of virus production (Figure 4E) and neutralization percentages (Figure 4F) were similar to that observed in Vero E6 cells. The IC50 for all VOCs was similar, except for Omicron BA.1 and BA.2 sub-variant for which it was even lower (Figure 4F) than the IC50 observed in Vero E6 cells (Figure 4C).

Thus, our hACE2.16 antibody efficiently neutralizes infection and inhibits virus production of all VOCs tested.

DISCUSSION

Omicron and its subvariants escape antibody responses thanks to their heavily mutated spike protein. Indeed, many cases of Omicron BA.1 reinfection were reported, either in recovered patients or in immunized individuals (Altarawneh et al., 2022; Pulliam et al., 2021).

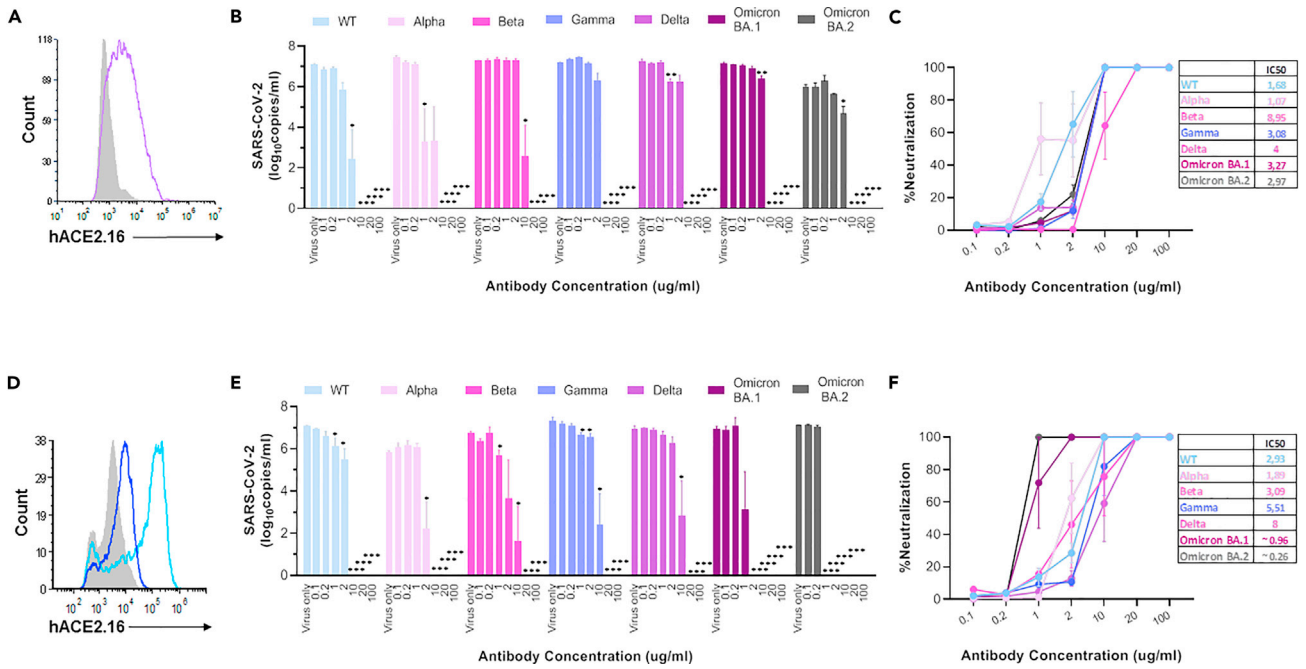

Figure 4. hACE2.16 inhibits SARS-CoV-2 VOCs infection and virus production

(A) FACS analysis of VERO E6 cells stained with hACE2.16 (purple). Gray histogram represent the background staining of 293T-ACE2 cells. Representative of 3 experiments.

(B) RT-qPCR analysis of supernatants obtained from the infected Vero E6 cells incubated with or without increasing concentrations of hACE2.16 antibody.

(C) %Neutralization was calculated using the results from B and IC50 (in ug/mL) was calculated from %Neutralization.

(D) FACS analysis of Calu-3 cells stained with hACE2.16 (light blue) or with commercial anti-ACE2 antibody (dark blue). Gray histogram represent the background staining of 293T-ACE2 cells incubated with secondary antibody only. Representative of 3 experiments.

(E) RT-qPCR analysis of supernatants obtained from the infected Calu-3 cells incubated with or without increasing concentrations of hACE2.16 antibody.

(F) % Neutralization was calculated using the results from E and IC50 (in ug/mL) was calculated from %Neutralization. (B and E). Copies/mL were calculated following the subtraction of the initial virus applied. *$p < 0.05$, **$p < 0.01$, ***$p < 0.0001$, Student's *t* test as compared to untreated cells (virus only). Data are mean ± SEM of 2-4 experiments.

As for vaccine protection, primary immunization with BNT162b2 or ChAdOx1 provided no or limited protection against symptomatic disease with Omicron BA.1 (Andrews et al., 2021).

Recent articles report that the Omicron variants BA.4 and even better escape from vaccine neutralization as compared to BA.1 and BA.2. ~2- to 3-fold reduction in neutralization titers was observed in vaccinated individuals as well as in BA.1 breakthrough infection (Tuekprakhon et al., 2022a).

BA.4 and 5 also show reduced sensitivity toward most of the current therapeutic monoclonal antibodies including bamlanivimab, casirivimab, etesevimab, imdevimab, tixagevimab (Yamasoba et al., 2022b), sotrovimab, casirivimab + imdevimab and bamlanivimab + etesivimab (NIH, 2022).

Apart from the current treatments that are already in use, ~50 monoclonal antibodies are in development (Renn et al., 2020), but practically all of them, target the spike protein, thus it may render them less efficient against the current VOC or future ones.

Only one team reported on a treatment that targets ACE2. They showed that the antibody they generated against ACE2 (called 3E8) could block pseudo-typed coronaviruses infections and suppress live Delta VOC infection in the lungs of BALB/c mice ectopically expressing human ACE2. But they have yet to report whether it is effective against Omicron subvariants (Chen et al., 2021; Ou et al., 2022).

We developed here an antibody hACE2.16, initially selected based on its ability to block RBD-Ig binding, that blocks ACE2-RBD interaction, consequently inhibiting SARS-CoV-2 cell entry and virus production.

We further demonstrated that hACE2.16 binding does not lead to ACE2 internalization nor that it interferes with ACE2 enzymatic activity. Indeed, it was reported that the RBD binding site does not overlap with the catalytic site of ACE2 (Kuba et al., 2005).

We observed 100% neutralization of SARS-CoV-2 various VOCs in VERO E6 cells (without TMPRSS2) as well as in Calu-3 cells (with TMPRSS2). In Vero E6 cells, infection with the Beta variant was less efficient as compared to other VOCs. However, this was not observed in Calu-3 cells. We consider the results obtained with Calu-3 cells as more reliable as it is a human lung epithelial cell line, while Vero-E6 cells are monkey kidney cells. In Calu-3 cells, infection with the Omicron subvariants BA.1 and BA.2 was most efficiently inhibited by our anti-ACE2 antibody. One possible explanation for this might be that Omicron inefficiently uses TMPRSS2, which mediates cell entry through plasma membrane fusion (Meng et al., 2022). Also, differences in TMPRSS2 dependence are suggested to be related to the furin cleavage site, which is different for the Omicron (P681H) and Delta variants (P681R) (Zhao et al., 2022).

To summarize, we demonstrated that hACE2.16 can efficiently block infection and virus production of all VOCs and we thus suggest that hACE2.16 might be an efficient treatment against all SARS-CoV-2 VOCs, the current ones and probably future ones.

Limitations of the study

Because new VOCs constantly appear we did not yet investigate whether infection with current Omicron variants BA.4, BA.5, and BA.2.75 is inhibited by our anti-ACE2 antibody. In addition, we still need to test whether our anti-ACE2 antibody will block infection *in vivo*. Antibody toxicity should also be examined.

STAR★METHODS

Detailed methods are provided in the online version of this paper and include the following:

- KEY RESOURCES TABLE
- RESOURCE AVAILABILITY
  - Lead contact
  - Materials availability
  - Data and code availability
- EXPERIMENTAL MODEL AND SUBJECT DETAILS
  - Cells and bacterial strains
  - Viral isolation
- METHOD DETAILS
  - Lentivirus production
  - ACE2-Ig generation
  - Immunization protocol
  - Generation of 293T-ACE2 cells
  - Flow cytometry
  - Enzymatic activity
  - Viral titration
  - SARS-CoV-2 micro-neutralization assay
  - Quantitative reverse transcriptase PCR
- QUANTIFICATION AND STATISTICAL ANALYSIS

ACKNOWLEDGMENTS

This work was supported by the following grants awarded to O.M.: the Israel Innovation Authority Kamin grant 62615, the German-Israeli Foundation for Scientific Research and Development grant 1412-414.13/2017, the ICRF professorship grant, the ISF Israel-China grant 2554/18, the MOST-DKFZ grant 3-14931, and the Ministry of Science and Technology grant 3-14764, by Integra Holdings LTD, By the Rothschild Foundation and by the Israel Science Foundation Moked grant 442-18. Graphical abstract was created with BioRender.com.

AUTHOR CONTRIBUTIONS

Conceptualization, O.M. and S.J.; Methodology, O.M., S.J., M.M., and D.W.; Investigation, A.E.C., I.B., P.K.B., N.A., L.K., O.A., I.K., and L.T.; Visualization, O.M. and A.E.C.; Funding acquisition, O.M. and S.J.;

Project administration, O.M.; Supervision, O.M.; Writing – original draft, O.M. and A.E.C.; Writing – review & editing, O.M. and A.E.C.

DECLARATION OF INTERESTS

A patent application has been submitted by Yissum, the Hebrew University Tech Transfer Company, based on these results.

Received: April 5, 2022
Revised: July 25, 2022
Accepted: August 10, 2022
Published: September 16, 2022

REFERENCES

Administration, D. (2020a). Pfizer COVID-19 Vaccine EUA Letter of Authorization Reissued 12 (FDA), p. 23.

Administration, D. (2020b). Moderna COVID-19 Vaccine EUA Letter of Authorization (FDA).

Altarawneh, H., Chemaitelly, H., Tang, P., Hasan, M.R., Qassim, S., Ayoub, H.H., Almukdad, S., Yassine, H.M., Benslimane, F.M., Al Khatib, H.A., et al. (2022). Protection afforded by prior infection against SARS-CoV-2 reinfection with the Omicron variant. Preprint at medRxiv. https://doi.org/10.1101/2022.01.05.22268782.

Andrews, N., Stowe, J., Kirsebom, F., Toffa, S., Rickeard, T., Gallagher, E., Gower, C., Kall, M., Groves, N., O'Connell, A.-M., et al. (2021). Effectiveness of COVID-19 vaccines against the Omicron (B.1.1.529) variant of concern. Preprint at medRxiv. https://doi.org/10.1101/2021.12.14.21267615.

Baden, L.R., El Sahly, H.M., Essink, B., Kotloff, K., Frey, S., Novak, R., Diemert, D., Spector, S.A., Rouphael, N., Creech, C.B., et al. (2021). Efficacy and safety of the mRNA-1273 SARS-CoV-2 vaccine. N. Engl. J. Med. *384*, 403–416. https://doi.org/10.1056/NEJMoa2035389.

Beck, A., and Reichert, J.M. (2011). Therapeutic Fc-fusion proteins and peptides as successful alternatives to antibodies. mAbs *3*, 415–416. https://doi.org/10.4161/mabs.3.5.17334.

Bestle, D., Heindl, M.R., Limburg, H., van Lam van, T., Pilgram, O., Moulton, H., Stein, D.A., Hardes, K., Eickmann, M., Dolnik, O., et al. (2020). TMPRSS2 and furin are both essential for proteolytic activation of SARS-CoV-2 in human airway cells. Life Sci. Alliance *3*, e202000786. https://doi.org/10.26508/LSA.202000786.

Cao, Y., Yisimayi, A., Jian, F., Song, W., Xiao, T., Wang, L., Du, S., Wang, J., Li, Q., Chen, X., et al. (2022). BA.2.12.1, BA.4 and BA.5 escape antibodies elicited by Omicron infection. Nature. https://doi.org/10.1038/s41586-022-04980-y.

Cathcart, A.L., Havenar-Daughton, C., Lempp, F.A., Ma, D., Schmid, M.A., Agostini, M.L., Guarino, B., iulio, J.D., Rosen, L.E., Tucker, H., et al. (2022). The dual function monoclonal antibodies VIR-7831 and VIR-7832 demonstrate potent in vitro and in vivo activity against SARS-CoV-2. Preprint at bioRxiv. https://doi.org/10.1101/2021.03.09.434607.

Chaouat, A.E., Achdout, H., Kol, I., Berhani, O., Roi, G., Vitner, E.B., Melamed, S., Politi, B., Zahavy, E., Brizic, I., et al. (2021). SARS-CoV-2 receptor binding domain fusion protein efficiently neutralizes virus infection. PLoS Pathog. *17*, e1010175. https://doi.org/10.1371/JOURNAL.PPAT.1010175.

Chen, Y., Zhang, Y.N., Yan, R., Wang, G., Zhang, Y., Zhang, Z.R., Li, Y., Ou, J., Chu, W., Liang, Z., et al. (2021). ACE2-targeting monoclonal antibody as potent and broad-spectrum coronavirus blocker. Signal Transduct. Target. Ther. *6*, 315. https://doi.org/10.1038/s41392-021-00740-y.

Dong, J., Zost, S.J., Greaney, A.J., Starr, T.N., Dingens, A.S., Chen, E.C., Chen, R.E., Case, J.B., Sutton, R.E., Gilchuk, P., et al. (2021). Genetic and structural basis for recognition of SARS-CoV-2 spike protein by a two-antibody cocktail. Preprint at bioRxiv. https://doi.org/10.1101/2021.01.27.428529.

Dougan, M., Nirula, A., Azizad, M., Mocherla, B., Gottlieb, R.L., Chen, P., Hebert, C., Perry, R., Boscia, J., Heller, B., et al. (2021). Bamlanivimab plus etesevimab in mild or moderate Covid-19. N. Engl. J. Med. https://doi.org/10.1056/NEJMoa2102685.

European Centre for Disease Prevention and Control (2022). Epidemiological update: SARS-CoV-2 omicron sub-lineages BA.4 and BA.5. https://www.ecdc.europa.eu/en/news-events/epidemiological-update-sars-cov-2-omicron-sub-lineages-ba4-and-ba5.

FDA (2022). Emergency Use Authorization | FDA (Food Drug Administration).

Group, R.C., Horby, P.W., Mafham, M., Peto, L., Campbell, M., Pessoa-Amorim, G., Spata, E., Staplin, N., Emberson, J.R., Prudon, B., et al. (2021). Casirivimab and imdevimab in patients admitted to hospital with COVID-19 (RECOVERY): a randomised, controlled, open-label, platform trial. Preprint at medRxiv. https://doi.org/10.1101/2021.06.15.21258542.

Gupta, A., Gonzalez-Rojas, Y., Juarez, E., Casal, M.C., Moya, J., Falci, D.R., Sarkis, E., Solis, J., Zheng, H., Scott, N., et al.; Investigators, for the C.-I (2021). Early Covid-19 treatment with SARS-CoV-2 neutralizing antibody sotrovimab. Preprint at medRxiv. https://doi.org/10.1101/2021.05.27.21257096.

Harper, S., and Speicher, D.W. (1997). Expression and purification of GST fusion proteins. Curr. Protoc. Protein Sci. *6*. 6.6.21. https://doi.org/10.1002/0471140864.PS0606S09.

Harvey, W.T., Carabelli, A.M., Jackson, B., Gupta, R.K., Thomson, E.C., Harrison, E.M., Ludden, C., Reeve, R., Rambaut, A.; COVID-19 Genomics UK COG-UK Consortium, and Robertson, D.L. (2021). SARS-CoV-2 variants, spike mutations and immune escape. Nat. Rev. Microbiol. *19*, 409–424. https://doi.org/10.1038/s41579-021-00573-0.

Kannan, S.R., Spratt, A.N., Sharma, K., Chand, H.S., Byrareddy, S.N., and Singh, K. (2022). Omicron SARS-CoV-2 variant: unique features and their impact on pre-existing antibodies. J. Autoimmun. *126*, 102779. https://doi.org/10.1016/J.JAUT.2021.102779.

Kuba, K., Imai, Y., Rao, S., Gao, H., Guo, F., Guan, B., Huan, Y., Yang, P., Zhang, Y., Deng, W., et al. (2005). A crucial role of angiotensin converting enzyme 2 (ACE2) in SARS coronavirus–induced lung injury. Nat. Med. *11*, 875–879. https://doi.org/10.1038/nm1267.

Laffeber, C., de Koning, K., Kanaar, R., and Lebbink, J.H.G. (2021). Experimental evidence for enhanced receptor binding by rapidly spreading SARS-CoV-2 variants. J. Mol. Biol. *433*, 167058. https://doi.org/10.1016/J.JMB.2021.167058.

Levin, M.J., Ustianowski, A., De Wit, S., Launay, O., Avila, M., Templeton, A., Yuan, Y., Seegobin, S., Ellery, A., Levinson, D.J., et al.; PROVENT Study Group (2022). Intramuscular AZD7442 (Tixagevimab–Cilgavimab) for prevention of Covid-19. N. Engl. J. Med. *386*, 2188–2200. https://doi.org/10.1056/nejmoa2116620.

Liu, L., Iketani, S., Guo, Y., Chan, J.F.-W., Wang, M., Liu, L., Luo, Y., Chu, H., Huang, Y., Nair, M.S., et al. (2021a). Striking antibody evasion manifested by the omicron variant of SARS-CoV-2. Nature *602*, 676–681. https://doi.org/10.1038/s41586-021-04388-0.

Liu, Y., Arase, N., Kishikawa, J., Hirose, M., Li, S., Tada, A., Matsuoka, S., Arakawa, A., Akamatsu, K., Ono, C., et al. (2021b). The SARS-CoV-2 Delta variant is poised to acquire complete resistance to wild-type spike vaccines. Preprint at bioRxiv. https://doi.org/10.1101/2021.08.22.457114.

Loganathan, S., Kuppusamy, M., Wankhar, W., Gurugubelli, K.R., Mahadevappa, V.H., Lepcha, L., and Choudhary, A.K. (2021). Angiotensin-converting enzyme 2 (ACE2): COVID 19 gate way

to multiple organ failure syndromes. Respir. Physiol. Neurobiol. *283*, 103548. https://doi.org/10.1016/j.resp.2020.103548.

Lu, L., Mok, B.W.-Y., Chen, L.-L., Chan, J.M.-C., Tsang, O.T.-Y., Lam, B.H.-S., Chuang, V.W.-M., Chu, A.W.-H., Chan, W.-M., Ip, J.D., et al. (2021). Neutralization of SARS-CoV-2 Omicron variant by sera from BNT162b2 or Coronavac vaccine recipients. Clin. Infect. Dis. ciab1041. https://doi.org/10.1093/CID/CIAB1041.

Lupala, C.S., Ye, Y., Chen, H., Su, X.-D., and Liu, H. (2022). Mutations on RBD of SARS-CoV-2 Omicron variant result in stronger binding to human ACE2 receptor. Biochem. Biophys. Res. Commun. *590*, 34–41. https://doi.org/10.1016/J.BBRC.2021.12.079.

Meng, B., Abdullahi, A., Ferreira, I.A.T.M., Goonawardane, N., Saito, A., Kimura, I., Yamasoba, D., Gerber, P.P., Fatihi, S., Rathore, S., et al. (2022). Altered TMPRSS2 usage by SARS-CoV-2 Omicron impacts infectivity and fusogenicity. Nature *603*, 706–714. https://doi.org/10.1038/s41586-022-04474-x.

Naldini, L., Blömer, U., Gallay, P., Ory, D., Mulligan, R., Gage, F.H., Verma, I.M., and Trono, D. (1996). In vivo gene delivery and stable transduction of nondividing cells by a lentiviral vector. Science *272*, 263–267. https://doi.org/10.1126/science.272.5259.263.

National Institutes of Health (2021). What's New | COVID-19 Treatment Guidelines (National Institutes of Health). https://www.covid19treatmentguidelines.nih.gov/about-the-guidelines/whats-new/.

NIH (2022). Anti-SARS-CoV-2 Monoclonal Antibodies | COVID-19 Treatment Guidelines (National Institutes of Health). COVID-19 Treat. Guidel. https://www.covid19treatmentguidelines.nih.gov/tables/variants-and-susceptibility-to-mabs/.

Ou, J., Zhang, Y., Wang, Y., Zhang, Z., Wei, H., Yu, J., Wang, Q., Wang, G., Zhang, B., and Wang, C. (2022). ACE2-Targeting antibody suppresses SARS-CoV-2 Omicron and Delta variants. Signal Transduct. Target. Ther. *7*, 43. https://doi.org/10.1038/s41392-022-00913-3.

Polack, F.P., Thomas, S.J., Kitchin, N., Absalon, J., Gurtman, A., Lockhart, S., Perez, J.L., Pérez Marc, G., Moreira, E.D., Zerbini, C., et al.; C4591001 Clinical Trial Group (2020). Safety and efficacy of the BNT162b2 mRNA Covid-19 vaccine. N. Engl. J. Med. *383*, 2603–2615. https://doi.org/10.1056/NEJMoa2034577.

Pulliam, J.R.C., Schalkwyk, C. van, Govender, N., Gottberg, A. von, Cohen, C., Groome, M.J., Dushoff, J., Mlisana, K., and Moultrie, H. (2021). Increased risk of SARS-CoV-2 reinfection associated with emergence of the Omicron variant in South Africa. Preprint at medRxiv. https://doi.org/10.1101/2021.11.11.21266068.

Renn, A., Fu, Y., Hu, X., Hall, M.D., and Simeonov, A. (2020). Fruitful neutralizing antibody pipeline brings hope to defeat SARS-Cov-2. Trends Pharmacol. Sci. *41*, 815–829. https://doi.org/10.1016/j.tips.2020.07.004.

Rössler, A., Riepler, L., Bante, D., von Laer, D., and Kimpel, J. (2022). SARS-CoV-2 omicron variant neutralization in serum from vaccinated and convalescent persons. N. Engl. J. Med. *386*, 698–700. https://doi.org/10.1056/NEJMC2119236/SUPPL_FILE/NEJMC2119236_DISCLOSURES.PDF.

Sheward, D.J., Kim, C., Ehling, R.A., Pankow, A., Castro Dopico, X., Dyrdak, R., Martin, D.P., Reddy, S.T., Dillner, J., Karlsson Hedestam, G.B., et al. (2022). Neutralisation sensitivity of the SARS-CoV-2 omicron (B.1.1.529) variant: a cross-sectional study. Lancet Infect. Dis. *22*, 813–820. https://doi.org/10.1016/S1473-3099(22)00129-3.

Tao, K., Tzou, P.L., Nouhin, J., Gupta, R.K., de Oliveira, T., Kosakovsky Pond, S.L., Fera, D., and Shafer, R.W. (2021). The biological and clinical significance of emerging SARS-CoV-2 variants. Nat. Rev. Genet. *22*, 757–773. https://doi.org/10.1038/s41576-021-00408-x.

Triposkiadis, F., Xanthopoulos, A., Giamouzis, G., Boudoulas, K.D., Starling, R.C., Skoularigis, J., Boudoulas, H., and Iliodromitis, E. (2021). ACE2, the counter-regulatory renin–angiotensin system Axis and COVID-19 severity. J. Clin. Med. *10*, 3885. https://doi.org/10.3390/JCM10173885.

Tuekprakhon, A., Huo, J., Nutalai, R., Dijokaite-Guraliuc, A., Zhou, D., Ginn, H.M., Selvaraj, M., Liu, C., Mentzer, A.J., Supasa, P., et al. (2022a). Further antibody escape by Omicron BA.4 and BA.5 from vaccine and BA.1 serum. Preprint at bioRxiv. https://doi.org/10.1101/2022.05.21.492554.

Tuekprakhon, A., Huo, J., Nutalai, R., Dijokaite-Guraliuc, A., Zhou, D., Ginn, H.M., Selvaraj, M., Liu, C., Mentzer, A.J., Supasa, P., et al. (2022b). Antibody escape of SARS-CoV-2 Omicron BA.4 and BA.5 from vaccine and BA.1 serum. Cell. https://doi.org/10.1016/J.CELL.2022.06.005.

U.S. Food and Drug Administration (2021). Fact Sheet for Healthcare Providers Emergency Use Authorization (EUA) for Paxlovid (U.S. Food and Drug Administration), pp. 1–29.

Wang, P., Casner, R.G., Nair, M.S., Wang, M., Yu, J., Cerutti, G., Liu, L., Kwong, P.D., Huang, Y., Shapiro, L., and Ho, D.D. (2021). Increased resistance of SARS-CoV-2 variant P.1 to antibody neutralization. Cell Host Microbe *29*, 747–751.e4. https://doi.org/10.1016/J.CHOM.2021.04.007/ATTACHMENT/030B3461-4CCE-4B20-91D2-17394C35C372/MMC1.PDF.

Wang, Q., Zhang, Y., Wu, L., Niu, S., Song, C., Zhang, Z., Lu, G., Qiao, C., Hu, Y., Yuen, K.Y., et al. (2020). Structural and functional basis of SARS-CoV-2 entry by using human ACE2. Cell *181*, 894–904.e9. https://doi.org/10.1016/j.cell.2020.03.045.

Wang, W., McKinnie, S.M.K., Farhan, M., Paul, M., McDonald, T., McLean, B., Llorens-Cortes, C., Hazra, S., Murray, A.G., Vederas, J.C., and Oudit, G.Y. (2016). Angiotensin-Converting enzyme 2 metabolizes and partially inactivates pyr-apelin-13 and apelin-17: physiological effects in the cardiovascular system. Hypertension *68*, 365–377. https://doi.org/10.1161/HYPERTENSIONAHA.115.06892.

Westendorf, K., Žentelis, S., Wang, L., Foster, D., Vaillancourt, P., Wiggin, M., Lovett, E., van der Lee, R., Hendle, J., Pustilnik, A., et al. (2022). LY-CoV1404 (bebtelovimab) potently neutralizes SARS-CoV-2 variants. Cell Rep. *39*, 110812. https://doi.org/10.1016/J.CELREP.2022.110812.

World Health Organization (2022). COVID-19 Weekly Epidemiological Update (World Health Organization), pp. 1–23.

Wu, J., Deng, W., Li, S., and Yang, X. (2021). Advances in research on ACE2 as a receptor for 2019-nCoV. Cell. Mol. Life Sci. *78*, 531–544. https://doi.org/10.1007/S00018-020-03611-X/FIGURES/4.

Yamasoba, D., Kimura, I., Nasser, H., Morioka, Y., Nao, N., Ito, J., Uriu, K., Tsuda, M., Zahradnik, J., Shirakawa, K., et al. (2022a). Virological characteristics of SARS-CoV-2 BA.2 variant. Preprint at bioRxiv. https://doi.org/10.1101/2022.02.14.480335.

Yamasoba, D., Kosugi, Y., Kimura, I., Fujita, S., Uriu, K., Ito, J., and Sato, K.; The Genotype to Phenotype Japan (G2P-Japan) Consortium (2022b). Sensitivity of novel SARS-CoV-2 Omicron subvariants, BA.2.11, BA.2.12.1, BA.4 and BA.5 to therapeutic monoclonal antibodies. Preprint at bioRxiv. https://doi.org/10.1101/2022.05.03.490409.

Zhang, L., Cui, Z., Li, Q., Yu, Y., Wu, J., Nie, J., Wang, H., Zhang, Y., Liu, S., Chen, Z., et al. (2021). Comparison of 10 emerging SARS-COV-2 variants: infectivity, animal tropism, and antibody neutralization. Res. Sq, 1–18.

Zhao, H., Lu, L., Peng, Z., Chen, L.L., Meng, X., Zhang, C., Ip, J.D., Chan, W.M., Chu, A.W.H., Chan, K.H., et al. (2022). SARS-CoV-2 Omicron variant shows less efficient replication and fusion activity when compared with Delta variant in TMPRSS2-expressed cells. Emerg. Microbes. Infect. *11*, 277–283. https://doi.org/10.1080/22221751.2021.2023329.

Zhou, L., Niu, Z., Jiang, X., Zhang, Z., Zheng, Y., Wang, Z., Zhu, Y., Gao, L., Huang, H., Wang, X., and Sun, Q. (2020). Systemic analysis of tissue cells potentially vulnerable to SARS-CoV-2 infection by the protein-proofed single-cell RNA profiling of ACE2, TMPRSS2 and Furin proteases. Preprint at bioRxiv. https://doi.org/10.1101/2020.04.06.028522.

STAR★METHODS

KEY RESOURCES TABLE

REAGENT or RESOURCE	SOURCE	IDENTIFIER
Antibodies		
Purified anti-DYKDDDDK Tag Antibody	BioLegend	Cat#637302
Angiotensin I Converting Enzyme 2 antibody (ACE2) Clone- AC18F	antibodies-online	#ABIN1169449
anti-hACE2.01-16	This paper	N/A
Peroxidase AffiniPure F(ab')2 fragment specific Goat Anti-Mouse IgG antibody	Jackson ImmunoResearch	Cat#115-036-072
Alexa Fluor 647-conjugated Goat Anti-Mouse IgG	Jackson ImmunoResearch	Cat#115-606-062
Bacterial and virus strains		
DH5α bacteria	Thermo Fisher Scientific	Cat#18258012
SARS-CoV-2 B.1.1.50 (hCoV-19/Israel/CVL-45526-ngs/2020	Isolated from patient	N/A
SARS-CoV-2 B.1.1.7 (hCoV-19/Israel/CVL-46879-ngs/2020)	Isolated from patient	N/A
SARS-CoV-2 B.1.351 (hCoV-19/Israel/CVL-2557-ngs/2020)	Isolated from patient	N/A
SARS-CoV-2 B.1.617.2 (hCoV-19/Israel/CVL-12804/2021)	Isolated from patient	N/A
SARS-CoV-2 B.1.1.529 (hCoV-19/Israel/CVL-n49814/2021)	Isolated from patient	N/A
SARS-CoV-2 Omicron BA.2 (hCoV-19/Israel/CVL-n51046/2022)	Isolated from patient	N/A
SARS-CoV-2 P.1	Profs. Ester Sabino and Maria Cassia Mendes Correa (Tropical Medicine Institute Sao Paulo University)	N/A
Chemicals, peptides, and recombinant proteins		
Mca-Y-V-A-D-A-P-K(Dnp)-OH fluorogenic peptide	R&D Systems	Cat#ES007
o-phenylenediamine dihydrochloride	Sigma	Cat#P8412
RBD-Ig	Chaouat et al., (2021)	N/A
ACE2-Ig	Chaouat et al., (2021)	N/A
Experimental models: Cell lines		
HEK-293T cells	ATCC	CRL-3216
VERO E6	ATCC	CRL-1586
Calu-3 cells	ATCC	HTB-55
293T-ACE2 cells	Chaouat et al., (2021)	N/A
Oligonucleotides		
293T-ACE2 generation: Primer FW reaction 1: AAATTGAATTCGCCGCCACCATG CCCATGGGGTCTCTGCA	Chaouat et al., (2021)	N/A
293T-ACE2 generation: Primer RV reaction 1: GTTGG TGATGTTTCCGAGGCAGGAAGCGACC	Chaouat et al., (2021)	N/A
Primer FW reaction 2: GCCTCGGAAACATCACC AACCTGTGTCCAT	Chaouat et al., (2021)	N/A
Primer RV reaction 2: TTTGGATCCACTGTG GCAGGGGCATGG	Chaouat et al., (2021)	N/A

(*Continued on next page*)

Continued

REAGENT or RESOURCE	SOURCE	IDENTIFIER
Primer FW for ACE2-Ig: AAAGCTAGCGCCGC CACCATGTCAAGCTCTTCCTGGC.	Chaouat et al., (2021)	N/A
Primer RV for ACE2-Ig: TTTTGATCAGAA ACAGGGGGCTG.	Chaouat et al., (2021)	N/A
Software and algorithms		
Prism8	GraphPad Software	https://www.graphpad.com/scientific-software/prism/
FCS Express 7	*De Novo* Software	https://denovosoftware.com/demo-overview/

RESOURCE AVAILABILITY

Lead contact

Further information and requests for resources and reagents should be directed to and will be fulfilled by the lead contact, Ofer Mandelboim (oferm@ekmd.huji.ac.il).

Materials availability

Newly generated materials reported in this paper are available from the lead contact upon request.

Data and code availability

Data reported in this paper will be shared by the lead contact upon request. This paper does not report original code. Any additional information required to reanalyze the data reported in this paper is available from the lead contact upon request.

EXPERIMENTAL MODEL AND SUBJECT DETAILS

Cells and bacterial strains

HEK-293T cells (ATCC, CRL-3216), 293T-ACE2 cells (generated by us), Calu-3 cells (ATCC, HTB-55) and VERO E6 (ATCC, CRL-1586) were cultured in Dulbecco's modified Eagle's medium (DMEM, Sigma-Aldrich) containing 10% Fetal bovine serum (FBS), (Sigma-Aldrich), 1% L-glutamine (Biological Industries (BI)), 1% sodium pyruvate (BI), 1% nonessential amino acids (BI), and 1% penicillin-streptomycin (BI).Cells were maintained at 37 °C with 5% CO2. DH5α bacteria (Thermo Fisher Scientific, 18,258,012) grown in LB media at 37°C were used for cloning and amplification of plasmid DNA for mammalian cell transfection.

Viral isolation

Using sequencing, we identified 5 nasopharyngeal samples from SARS-CoV-2 positive individuals which contained the Wild Type sub lineage B.1.1.50 (hCoV-19/Israel/CVL-45526-ngs/2020), Alpha, B.1.1.7 (hCoV-19/Israel/CVL-46879-ngs/2020), Beta B.1.351 (hCoV-19/Israel/CVL-2557-ngs/2020), Delta, B.1.617.2 (hCoV-19/Israel/CVL-12804/2021), Omicron BA.1, B.1.1.529 (hCoV-19/Israel/CVL-n49814/2021), Omicron BA.2 (hCoV-19/Israel/CVL-n51046/2022) variants. Confluent VERO-E6 cells were incubated for 1 h at 33ºC with 300μL of nasopharyngeal samples followed by addition of 2% FBS to MEM-EAGLE medium. Upon CPE detection, supernatants were aliquoted and stored at −80ºC. Isolation of the P.1 (Gamma) variant was generously obtained from Profs. Ester Sabino and Maria Cassia Mendes Correa from Tropical Medicine Institute Sao Paulo University (Brazil).

METHOD DETAILS

Lentivirus production

Lentiviral vectors were produced by transient three-plasmid transfection as described here (Naldini et al., 1996). First, 293T cells were grown overnight in 6-well plates (2.2X105 cells/well). The following day pMD.G/VSV-G/SARS-CoV-2 spike envelope expressing plasmid (0.35 μg/well), a gag-pol packaging construct (0.65 μg/well) and the relevant vector construct (1 μg/well) were transfected using the TransIT-LT1 Transfection Reagent (MIR 2306, Mirus). Two days after transfection the soups containing the viruses were collected and filtered.

ACE2-Ig generation

PCR-generated fragments encoding the extracellular part of human ACE2 were cloned into a vector containing the Fc portion of human IgG1, and a Puromycin resistance gene. The Ig-vector was then introduced to 293T cells. Transfected cells were grown in the continuous presence of Puromycin. The ACE2-Ig fusion proteins secreted to the medium were purified on HiTrap Protein G High Performance column (Cat#GE17-0405-01, GE Healthcare).

Primer FW for ACE2-Ig: AAAGCTAGCGCCGCCACCATGTCAAGCTCTTCCTGGC.

Primer RV for ACE2-Ig: TTTTGATCAGAAACAGGGGGCTG.

Immunization protocol

Two BALB/c mice were immunized subcutaneously (s.c.) with 50 ug purified ACE2-Ig per mouse in Freund's complete adjuvant. Two weeks later mice were boosted with ACE2-Ig in Freund's incomplete adjuvant. Blood was collected from the tail vein 15 days after the second immunization and serum was subjected to enzyme-linked immunosorbent assay (ELISA) to check antibody titer. Serum from non-immunized mouse was used as a control. Mice were then boosted with ACE2-Ig (in PBS), i.v. and euthanized after 3 days. Splenocytes were isolated and subjected to fusion with SP2/O myeloma cells (ratio 1:1). Cells were cultivated in 96-well plates in 20% RPMI 1640 medium with hypoxanthine, aminopterin, and thymidine (HAT) used for hybridoma selection. Hybridoma cultures were screened for the production of antibodies using ELISA. In brief, 2 ug/mL of ACE2-Ig or negative control protein (hFc) was coated on high-binding ELISA plates (MICROLON High Binding, Greiner Bio-One, Kremsmünster, Austria) in carbonate/bicarbonate coating buffer pH 9.6. Plates were incubated overnight at 2–8 C, washed and saturated with blocking buffer (2.5 g BSA in 1000 mL demineralized water with 50 uL Tween 20 and 5 mL 10% azide for 2 h at room temperature. Hybridoma supernatants were added in PFT buffer (PBS containing 1% FBS and 0.05% Tween 20) diluted 1:2. After 1–2 h sample incubation, plates were washed and incubated for 1h with Peroxidase AffiniPure F(ab')2 fragment specific Goat Anti-Mouse IgG antibody (Jackson ImmunoResearch, West Grove, PA, USA, 115-036-072) diluted 1:2000 in PFT. After washing, a colorimetric reaction was performed with a 0.6 mg/mL solution of *o*-phenylenediamine dihydrochloride (OPD) (Sigma, Cat#P8412) in citrate buffer pH 5.5 and 0.001% of 30% hydrogen peroxide at RT for 5–10 min. After stopping the reaction with 1 M sulfuric acid, the absorbance was measured using a Tri-Star LB 941 multimode microplate reader with the wavelength set at 490 nm and the reference filter set at 630 nm. Positive hybridomas were cloned. The Animal Welfare Committee at the University of Rijeka, Faculty of Medicine and National ethics committee at Croatian Ministry of Agriculture approved all animal experiments (525-10/0543-20-3).

Generation of 293T-ACE2 cells

ACE2 was amplified from cDNA and an N-terminal FLAG Tag was introduced immediately after ACE2 signal peptide. This insert was then cloned into the plasmid pHAGE- dsRed (–) GFP (+). This plasmid carrying the insert was used as a vector construct to produce lentiviruses. The resulting lentiviruses were used to infect 293T cells. The transduced cells were checked for GFP expression using Flow Cytometry. PCR-generated fragments were made from 2 separated PCR reactions followed by a third reaction in which we used the forward primer of reaction 1, the reverse primer of reaction 2 and the products from reaction 1 and 2 as a template.

Primer FW reaction 1: AAATTGAATTCGCCGCCACCATGCCCATGGGGTCTCTGCA. Primer RV reaction 1: GTTGGTGATGTTTCCGAGGCAGGAAGCGACC.

Primer FW reaction 2: GCCTCGGAAACATCACCAACCTGTGTCCAT.

Primer RV reaction 2: TTTGGATCCACTGTGGCAGGGGCATGG.

Flow cytometry

Staining of the different cell types with either anti-hACE2.01-16 (generated by us)/Purified anti-DYKDDDDK Tag Antibody (Cat#637302, BioLegend), /commercial anti-hACE2 (#ABIN1169449, antibodies-online) were performed at 4 °C for 1 h, cells were then washed in FACS buffer (1% BSA and 0.05% Sodium Azide in PBS) and secondary antibody (Alexa Fluor 647-conjugated Goat Anti-Mouse IgG, Cat#115-606-062, Jackson

ImmunoResearch Laboratories) was added for 30 min at 4 °C. Then, cells were washed in FACS buffer followed by CytoFlex analysis. Data were analyzed using FCS Express 6/7.

Enzymatic activity

ACE2 enzymatic activity assay was performed in 96F plates. First 3M of 293T-ACE2 cells were lyzed from which 10ug/well was incubated with 1ug/well of antibody or without followed by a 15 min incubation. After incubation Mca-Y-V-A-D-A-P-K(Dnp)-OH fluorogenic peptide substrate was added and plate immediately read. The assay was performed with an ACE2 assay buffer containing 1M NaCl with 75mM Tris (pH 7.5). Fluorescence (Ex/Em 320/420 nm) was measured in a kinetic mode at room temperature. Plates were read by Tecan Spark 10M and data were analyzed using Magellan 1.1.

Viral titration

In order to calibrate and determine the 50% endpoint titer (TCID50) of each variant VERO-E6 cells at a concentration of 20*10^3/well, were seeded in 96-wells plates with 10% FBS MEM-EAGLE medium, and stored at 37ºC for 24 h. 10-fold serial dilutions of each variant were prepared using 2% FBS MEM-EAGLE medium and incubated for five days with the VERO-E6 cells. Following Gentian Violet staining, TCID50 of each variant was calculated using the Spearman-Karber method.

SARS-CoV-2 micro-neutralization assay

VERO-E6 cells at concentration of 20*103/well were seeded in sterile 96-wells plates with 10% FCS MEM-EAGLE medium and stored at 37ºC for 24 h. VERO-E6 cells pre-incubated with either anti-hACE2.16 (5-0.005μg/well) or 5μg/well of a control antibody, for 30 min at 33°C. One hundred TCID50 of Wild Type, Alpha, Beta, Gamma, Delta, and Omicron (BA.1 and BA.2) SARS-CoV-2 variants were used for infection. Plates were incubated for five days at 33°C after which supernatant was collected for RT-qPCR analysis.

Quantitative reverse transcriptase PCR

Nucleic acids were extracted using the MagNA Pure 96 Instrument (Roche Life Science), according to the manufacturer's instructions. Reverse transcription polymerase chain reactions (RT-PCRs) were performed using primers corresponding to the SARS-CoV-2 envelope (E) gene. Quantitative RT-PCR (qRT-PCR) was performed in 25 μL SensiFast reaction mix (Bioline, USA) using TaqMan Chemistry on a CFX-96 instrument.

QUANTIFICATION AND STATISTICAL ANALYSIS

Statistical analyses were performed using either Prism 8 (GraphPad) or Excel (Microsoft). *$p < 0.05$, **$p < 0.01$, ***$p < 0.0001$, Student's *t* test. Error bars represent SEM.